COMPARATIVE STUDY OF THE THERMAL STABILITY OF THE EPOXY SYSTEMS BADGE $n=0/1, 2$ DCH AND BADGE $n=0/1, 2$ DCH/CaCO$_3$

M. R. Núñez, M. Villanueva, B. Rial and L. Núñez[*]

Research Group TERBIPROMAT, Departamento de Física Aplicada, Facultad de Física, Universidade de Santiago de Compostela (USC) 15782, Santiago de Compostela, Spain

Abstract

The thermal degradation of the epoxy systems diglycidyl ether of bisphenol A (BADGE $n=0$)/1, 2 diamine cyclohexane (DCH) and diglycidyl ether of bisphenol A (BADGE $n=0$)/1, 2 diamine cyclohexane (DCH) containing calcium carbonate filler immersed and not immersed in hydrochloric acid have been studied by thermogravimetric analysis in order to compare their decomposition processes and to determine the reaction mechanism of the degradation processes. The value of the activation energies, necessary for this study, were calculated using various integral and differential methods. Analysis of the results suggests that hydrochloric acid does not affect the decomposition of the epoxy network and that the reaction mechanisms produce sigmoidal-type curves for the systems not immersed in HCl and deceleration curves for the same systems immersed.

Keywords: activation energy, epoxy resins, reaction mechanisms, thermogravimetry

Introduction

Thermosets are materials with low tensile and storage moduli. In many cases, it is necessary to add other components to the resin in order to improve its properties and/or to lower the prices of the final material. One of these components is an inert filler, CaCO$_3$, which does not change significantly the curing kinetic parameters of the two-component epoxy system studied, in our case BADGE $n=0/1, 2$ DCH, but can vary its mechanical properties, life-time, and thermal degradation kinetics.

Since the behavior of thermosets can be affected by the addition of fillers, it is important to investigate the changes that take place during the thermal degradation of these materials. The study of the degradation of a polymer is important because it can determine the upper temperature limit, the mechanism of a solid state process, and the life-time for a thermoset.

One of the main applications of epoxy materials in industry is in the production of different types of protective coating. So, in this work, the behaviour of the above-

[*]   Author for correspondence: Phone/Fax: +34-981-524-350, E-mail: falisar1@uscmail.usc.es

mentioned epoxy system was studied with the aim of considering its potential use as a coating for a basin containing municipal waste, in which a common component is ion Cl$^-$. The addition of calcium carbonate filler to the epoxy system BADGE n=0/1, 2 DCH can reduce the price of the end-epoxy resin. This is one of the reasons why it is important to study the influence of this filler on the properties of the two-component system.

The main objective of this work was to compare the kinetics of thermal degradation of an epoxy resin with and without an inert filler (CaCO$_3$) and not immersed and immersed in hydrochloric acid in non-isothermal conditions.

Kinetic methods

Kinetic information can be extracted from dynamic experiments and kinetic parameters, which can be determined using a large number of differential and integral methods, depending mainly on the treatment of experimental data.

The rate of conversion, $d\alpha/dt$, is a linear function of a temperature-dependent rate constant and a temperature-independent function:

$$\frac{d\alpha}{dt} = kf(\alpha) \tag{1}$$

If we consider an Arrhenius-type dependence on temperature and if the temperature of the sample is changed by a controlled and constant heating rate, β, we can express the variation in the degree of conversion by the following equation:

$$\frac{d\alpha}{dT} = \frac{A}{\beta} e^{-E/RT} f(\alpha) \tag{2}$$

Integration of this equation from an initial temperature, T_0, corresponding to a zero degree of conversion, to the peak temperature of the derivative thermogravimetric curve (DTG), T_p, where $\alpha=\alpha_p$ gives [1]:

$$g(\alpha) = \int_0^{\alpha_p} \frac{d\alpha}{f(\alpha)} = \frac{A}{\beta} \int_0^{T_p} e^{-E/RT} dT \tag{3}$$

where $g(\alpha)$ is the integral function of conversion. To derive Eq. (3), it was assumed that there is no reaction between 0 and T_0. Several kinetic models have been proposed and these are shown in Table 1, together with the form of $g(\alpha)$ used [2–5].

In the case of polymers, this integral function, $g(\alpha)$, is either a sigmoidal function or a deceleration function. These functions were satisfactorily employed for the estimation of the reaction solid state mechanism from non-isothermal TG experiments [6]. The model associated with the best fit of a given set of TG data with Eq. (3), hence specifies the mechanism and yields the relevant kinetic parameters. To facilitate discussion and comparison, the kinetic analysis of thermogravimetric data was made following two different categories of methods: differential and integral methods.

Differential method

Analysis of the changes in thermogravimetric data brought about by variation of the heating rate, β, is the basis of the most powerful differential methods for the determination of kinetic parameters.

Kissinger's method [7]

Kissinger's method has been used in literature to determine the activation energy of solid state reactions from plots of the logarithms of the heating rate *vs*. the inverse of temperature at the maximum of the reaction rate in constant heating rate experiments.

The activation energy can be calculated by Kissinger's method without a precise knowledge of the *n*th order reaction mechanism, using the following equation:

$$\ln\frac{\beta}{T_{max}^2} = \left\{ \ln\frac{AR}{E} + \ln[n(1-\alpha_{max})^{n-1}] \right\} - \frac{E}{RT_{max}} \tag{4}$$

where β is the heating rate, T_{max} is the temperature corresponding to the inflection point of the thermodegradation curves which corresponds to the maximum reaction rate, *A* is the pre-exponential factor, α_{max} is the maximum conversion and *n* is the reaction order. This method is only good for a narrow temperature range around the maximum temperature.

Integral methods

The integral methods involve an approximate integration of Eq. (3). The methods discussed in the present paper are Flynn–Wall–Ozawa and Coats–Redfern.

Flynn–Wall–Ozawa method [8, 9]

Equation (3) is integrated using Doyle approximation [10]. The result of the integration after taking logarithms is:

$$\log\beta = \log\left[\frac{AE}{g(\alpha)R}\right] - 2.315 - \frac{0.457E}{RT} \tag{5}$$

where β, *A*, *E* and *T* have the known meanings.

This is one of the integral methods that can determine the activation energy without the knowledge of the reaction order. For this reason, it is used to determine the activation energy at given values of conversion, and for a wider temperature range than the one used by Kissinger.

Coats–Redfern method [11]

Coats–Redfern used an asymptotic approximation for resolution of Eq. (5) obtaining:

$$\ln\frac{g(\alpha)}{T^2} = \ln\frac{AR}{\beta E} - \frac{E}{RT} \tag{6}$$

The different degradation processes ($g(\alpha)$) are listed in Table 1.

Table 1 Algebraic expressions for $g(\alpha)$ for the most frequently used mechanisms of solid state processes

Symbol	$g(\alpha)$	Solid state processes
	Sigmoidal curves	
A_2	$[-\ln(1-\alpha)]^{1/2}$	nucleation and growth (Avrami equation 1)
A_3	$[-\ln(1-\alpha)]^{1/3}$	nucleation and growth (Avrami equation 2)
A_4	$[-\ln(1-\alpha)]^{1/4}$	nucleation and growth (Avrami equation 3)
	Deceleration curves	
R_1	α	phase boundary controlled reaction (one-dimensional movement)
R_2	$[1-(1-\alpha)^{1/2}]$	phase boundary controlled reaction (contracting area)
R_3	$[1-(1-\alpha)^{1/3}]$	phase boundary controlled reaction (contracting volume)
D_1	α^2	one-dimensional diffusion
D_2	$(1-\alpha)\ln(1-\alpha)+\alpha$	two-dimensional diffusion
D_3	$[1-(1-\alpha)^{1/3}]^2$	three-dimensional diffusion (Jander equation)
D_4	$(1-2/3\alpha)-(1-\alpha)^{2/3}$	three-dimensional diffusion (Ginstling–Brounshtein equation)
F_1	$-\ln(1-\alpha)$	random nucleation with one nucleus on the individual particle
F_2	$1/(1-\alpha)$	random nucleation with two nuclei on the individual particle
F_3	$1/(1-\alpha)^2$	random nucleation with two nuclei on the individual particle

Criado *et al.* [3] method for determination of reaction mechanism

The activation energy of a solid state reaction can be determined from several non-isothermal measurements whatever the reaction mechanism is. If the value of the activation energy is known, the kinetic model of the process can be found defining a function

$$Z(\alpha) = \frac{d\alpha/dt}{\beta} \Pi(x)T \tag{7}$$

where $x=E/RT$ and $\Pi(x)$ is an approximation of the temperature integral which cannot be expressed in a simple analytical form. In this study, we used the fourth rational expression of Senum and Yang [12] which gives errors lower than 10^{-5}% for $x=20$.

Combination of Eqs (1) and (7) gives:

$$Z(\alpha) = f(\alpha)\, g(\alpha) \qquad (8)$$

This latter equation was used to obtain the master curves as functions of the reaction degree corresponding to the different models listed in Table 1.

Plotting the $Z(\alpha)$ function calculated using both experimental data and Eq. (7), and comparing with the master curves leads to determine the mechanisms of solid state processes.

Experimental

Materials

The thermosetting sytems used were a stoichiometric mixture of epoxy resin and diamine, and then a 20% in mass of filler was added in the case of the system BADGE $n=0/1, 2$ DCH/$CaCO_3$. In this latter case, epoxy resin and inert filler were carefully and homogeneously mixed before being added to an amount of diamine equivalent to the epoxy curing agent stoichiometric ratio.

The epoxy resin was a commercial BADGE ($n=0$) (Resin 332, Sigma Chemical Co. Sant Louis, USA) with an equivalent molecular mass of 173.6 g/eq, as determined by wet analysis [13, 14]. The curing agent was 1, 2 diaminecyclohexane (DCH) (Fluka, Switzerland) with an amine hydrogen equivalent mass of 28.5. The inert filler was calcium carbonate (Analema, Spain).

Sample preparation

For the system BADGE $n=0/1, 2$ DCH epoxy resin and diamine were homogeneously mixed. The curing reaction, according to TTT diagram [15] of this material occurs in two stages: a first step 24 h at room temperature and a second one 16 h at 70°C.

For the other system, an amount of inert filler equivalent to 20% of the stoichiometric two-component system mass (epoxy, diamine) was added. This amount was found to be optimum through scanning electronic microscopy (SEM) and curing kinetics studies on these system using different amounts of the inert filler [16]. The kinetic study was made using different percentages of filler in the range from 10 to 30%. Three DSC dynamic experiments were performed at each concentration, and it was found that the only reproducible results were those corresponding to 20% of filler. To corrobate this results, we used a scanning electronic microscope to take micrograph images of the different samples. Again, samples with 20% of filler showed good homogeneity over the whole surface, while samples with other filler contents presented certain heterogeneity that make the reaction mechanism depend on the position of the filler in the network [16].

The curing reaction was programmed according to a TTT diagram specifically calculated for this material [17]. It consists of two stages: a first step of 67 min at 50°C and a second one of 18 h at 85°C in an oven. After curing, the samples were removed from the cylindrical frame.

For thermogravimetric analysis, the samples were cut in the form of 15–25 mg in mass and 6 mm in diameter discs. Once cut, some samples were immersed in HCl for 30 days.

Thermogravimetric analysis was performed using a Thermogravimetric Analyzer (TGA7) from Perkin Elmer controlled by a 1020 computer. The system was operated in the dynamic mode in the temperature range 50–900°C, at different heating rates: 5, 15, 25, 35 and 45°C min^{-1}.

All the experiments were carried out under a dry nitrogen atmosphere. The TGA7 analyzer requires two purge lines: one to purge the balance chamber and a second one to purge the sample-furnace area. After various experiments, it was found that the optimum gas flow rates were: 25 mL min^{-1} for the balance purge gas and 35 mL min^{-1} for the sample purge gas.
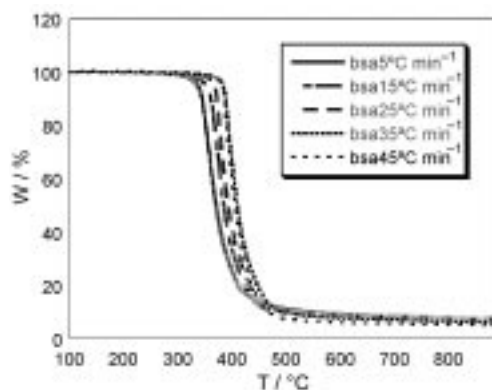

Fig. 1 Thermogravimetric curves of BADGE *n*=0/1, 2 DCH
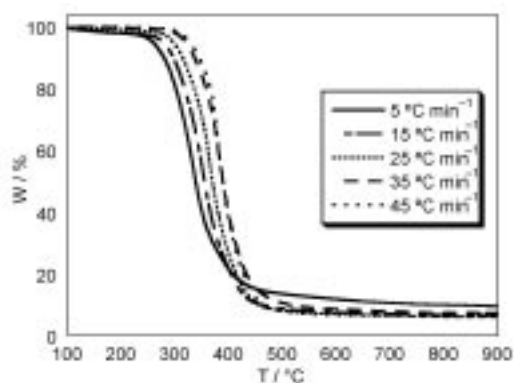

Fig. 2 Thermogravimetric curves of BADGE *n*=0/1, 2 DCH (30 days in HCl)

Results and discussion

Figures 1 and 2 show thermal degradation curves corresponding to dynamic experiments carried out on the system BADGE $n=0/1$, 2 DCH, at different heating rates: 5, 15, 25, 35 and 45°C min^{-1} before and after being immersed in HCl for 30 days [18, 19], respectively. These curves are C type [3], which correspond to a one-stage decomposition reaction where the procedural decomposition temperatures (initial and final) are well defined. The initial temperature represents the lowest temperature at which the onset of mass loss can be detected, and the final temperature represents the lowest temperature by which the process responsible for the mass change has been completed. Pérez-Maqueda *et al.* [23] studied the thermodegradation of $CaCO_3$ under high vacuum and found that follows a R_3 model after being immersed in HCl.

Figures 3 and 4 show decomposition curves corresponding to the system with filler not immersed and immersed in hydrochloric acid [20, 21], respectively. These
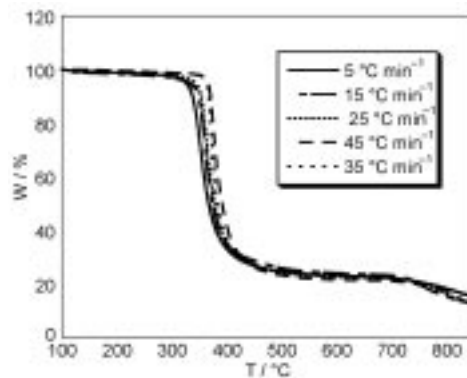

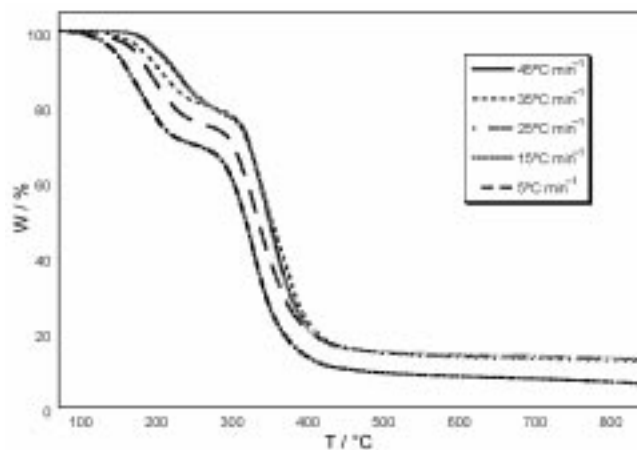**Fig. 3** Thermogravimetric curves of BADGE $n=0/1$, 2 DCH/$CaCO_3$

Fig. 4 Thermogravimetric curves of BADGE $n=0/1$, 2 DCH/$CaCO_3$ (30 days in HCl)

curves are D type [3], which correspond to a two-stage decomposition reaction. In Fig. 3, the first step is due to the thermal degradation of the epoxy resin and the second step corresponds to the degradation of the calcium carbonate (around 825°C). The thermogravimetric curves of the system BADGE $n=0/1$, 2 DCH/CaCO$_3$ immersed during 30 days in HCl show a first step due to dehydration of CaCl$_2$·6H$_2$O (around 200°C) and a second step that corresponds to the thermal degradation of the epoxy network. However, taking into account that samples were 1 mm width, it can be considered that the degradation takes place on the surface of the material.

Because of that, the internal structure of the epoxy network was affected neither by calcium carbonate filler nor by the hydrochloric acid [19, 21].

Owing to the thermodegradation behavior of the epoxy system studied here, we have chosen 10°C min^{-1} heating rates intervals, instead of 5°C min^{-1} intervals used by some authors [5, 18, 22], to avoid the overlapping of inflection point temperatures.

The inflection point temperature, T_m, necessary to calculate activation energies using Kissinger's method, can be determined from the minimum of the derivative of
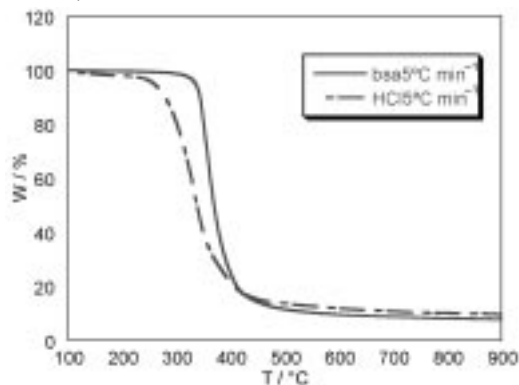

Fig. 5 Comparison of thermodegradation curves corresponding to the epoxy system BADGE $n=0/1$, 2 DCH not immersed and after 30 days of immersion in HCl
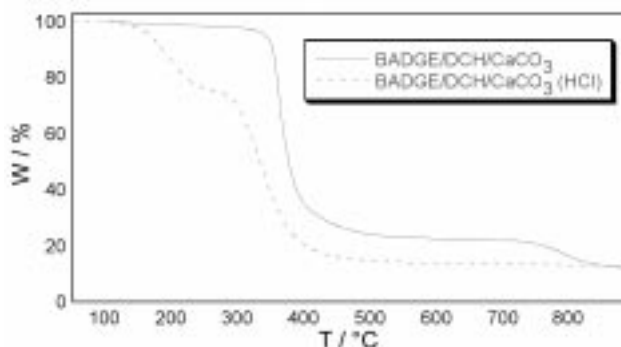

Fig. 6 Comparison of thermodegradation curves corresponding to the epoxy system BADGE $n=0/1$, 2 DCH/CaCO$_3$ not immersed and after 30 days of immersion in HCl

the thermal degradation curves. T_m is the temperature at which the maximum rate of degradation occurs.

Using Eq. (6) and the inflection point temperatures corresponding to the curves shown in Figs 1, 2, 3 and 4, respectively, the activation energies can be calculated from a plot of $\ln(\beta/T_{max}^2)$ *vs*. $1000/T_{max}$ and fitting to a straight line [18–21].

The activation energy can also be determined using the method of Flynn–Wall–Ozawa, Eq. (5), from a linear fitting of $\ln\beta$ *vs*. $1000/T$ at different conversions. Owing to the fact that this equation was derived using Doyle approximation, only some conversion ranges can be used: 5–20% for the systems without filler, 20–35% for the system BADGE n=0/1, 2 DCH/CaCO$_3$ and 35–50% for the latter system immersed in HCl [18–21].

Compared to others, these two methods present the advantage that they do not require the previous knowledge of the reaction mechanism for determining the activation energy. Some authors [5, 18] used the activation energies obtained using these two methods in order to check their thermodegradation mechanism models.

Table 2 shows activation energies obtained using Kissinger and Flynn–Wall–Ozawa methods. Analysis of this table shows that the values of the activation energies calculated using both methods are very similar for each of the systems not immersed in HCl. However, these values widely differ for each of the systems after being immersed in hydrochloric acid. This may be due to the fact that Kissinger's method does not account for the shape of the curve, as it concentrates on the inflection point temperature. On the contrary, the Flynn–Wall–Ozawa method does take the shape of the curve into account as it considers the whole range of degradation within the Doyle approximation. In Figs 5 and 6 degradation curves of the systems immersed and not immersed in HCl are compared. Figure 5 corresponds to the epoxy system without filler, while Fig. 6 corresponds to the three-component system. For this reason, the mean activation energies calculated using this latter method were taken as reference for discussion.

Table 2 Activation energies obtained using Kissinger and Flynn–Wall–Ozawa methods

	$(E_a)_{Kissinger}$/kJ mol^{-1}	$(E_a)_{Flynn-Wall-Ozawa}$/kJ mol^{-1}
BADGE n=0/1, 2 DCH	144.01	148.59±4.36
BADGE n=0/1, 2 DCH (30 days in HCl)	130.59	81.91±2.30
BADGE n=0/1, 2 DCH/CaCO$_3$	234.84	223.55±8.71
BADGE n=0/1, 2 DCH/CaCO$_3$ (30 days in HCl)	175.68	81.48±4.71

One other thing to be pointed out is the fact that the mean values of the activation energies for the two- and three-component systems immersed in HCl are very close, which could be justified by the fact that thermodegradation of the network, after being attacked by the acid, is not affected by the presence of CaCO$_3$. For samples practically 1 mm thick, as those used in the present study, all the filler reacts with HCl and,

because of this, the internal structure of the system immersed in the hydrochloric acid does not significantly change.

Table 3 Activation energies (kJ mol^{-1}) obtained using Coats–Redfern's method in the range 5–20% for different heating rates 5 to 45°C min^{-1} for the system BADGE n=0/1, 2 DCH

Mechanism	Heating rate/°C min^{-1}				
	5	15	25	35	45
A$_2$	294.41	299.77	447.36	486.85	536.56
A$_3$	192.89	196.41	294.64	320.94	354.15
A$_4$	142.08	144.42	218.08	238.25	262.65
R$_1$	564.99	574.13	851.38	927.12	1020.26
R$_2$	582.22	591.75	877.50	955.57	1051.65
R$_3$	588.11	597.59	886.25	965.21	1062.24
D$_1$	1139.81	1158.82	1717.21	1864.87	2051.78
D$_2$	1162.96	1181.87	1747.64	1902.81	2092.86
D$_3$	1186.54	1205.61	1783.03	1941.47	2135.31
D$_4$	1170.69	1189.97	1759.74	1915.49	2107.36
F$_1$	598.97	609.67	905.12	984.59	1083.80
F$_2$	18.78	17.53	97.23	106.95	118.42
F$_3$	37.56	35.15	205.17	224.79	247.80

Table 4 Activation energies (kJ mol^{-1}) obtained using Coats–Redfern's method in the range 5–20% for different heating rates 5 to 45°C min^{-1} for the system BADGE n=0/1, 2 DCH immersed for 30 days in HCl

Mechanism	Heating rate/°C min^{-1}				
	5	15	25	35	45
A$_2$	35.58	40.50	45.62	52.54	35.58
A$_3$	20.71	23.85	27.16	31.68	20.71
A$_4$	13.26	15.52	17.92	21.25	74.12
R$_1$	75.25	84.83	94.73	108.00	105.72
R$_2$	77.73	87.61	97.83	111.52	109.18
R$_3$	78.57	88.55	98.89	112.72	110.35
D$_1$	159.46	179.11	199.22	226.04	221.73
D$_2$	162.73	182.78	203.32	230.69	226.27
D$_3$	166.11	186.55	207.55	235.47	230.97
D$_4$	163.86	184.03	204.73	232.28	227.84
F$_1$	80.22	90.45	101.02	115.13	12.71
F$_2$	1.21	2.04	3.09	4.54	3.99
F$_3$	11.48	13.53	15.96	19.12	18.29

Table 5 Activation energies (kJ mol^{-1}) obtained using Coats–Redfern's method in the range
20–35% for different heating rates 5 to 45°C min^{-1} for the system BADGE n=0/1, 2
DCH/CaCO$_3$

Mechanism	Heating rate/°C min^{-1}				
	5	15	25	35	45
A$_2$	158.39	191.55	206.42	267.83	394.89
A$_3$	102.21	123.57	133.21	172.76	254.70
A$_4$	74.12	89.58	96.56	125.31	184.65
R$_1$	276.64	334.39	360.40	467.35	689.06
R$_2$	301.15	364.61	392.31	508.99	750.31
R$_3$	309.63	374.28	403.45	523.36	771.58
D$_1$	563.50	681.09	734.10	951.99	1403.56
D$_2$	595.20	719.56	775.49	1005.93	1483.00
D$_3$	629.40	760.81	819.95	1063.76	1568.26
D$_4$	606.55	733.36	790.36	1025.29	1511.51
F$_1$	203.01	395.47	426.22	553.03	815.21
F$_2$	96.40	116.84	125.81	163.96	241.40
F$_3$	327.08	246.06	264.84	345.20	508.32

Table 6 Activation energies (kJ mol^{-1}) obtained using Coats–Redfern's method in the range
35–50% for different heating rates 5 to 45°C min^{-1} for the system BADGE n=0/1, 2
DCH/CaCO$_3$ immersed for 30 days in HCl

Mechanism	Heating rate/°C min^{-1}				
	5	15	25	35	45
A$_2$	61.01	39.91	51.48	62.07	62.04
A$_3$	61.01	35.01	51.48	62.07	62.04
A$_4$	61.01	35.01	51.48	62.07	62.04
R$_1$	43.40	24.61	36.17	44.01	43.98
R$_2$	6.04	0.49	3.70	5.87	5.82
R$_3$	0.42	3.67	1.91	0.74	0.79
D$_1$	96.41	58.81	82.25	98.16	98.17
D$_2$	107.01	65.60	91.46	109.03	109.04
D$_3$	8.77	2.24	6.07	8.67	8.62
D$_4$	71.55	68.18	94.95	113.15	113.15
F$_1$	61.01	35.91	51.48	62.07	62.04
F$_2$	29.21	15.29	23.84	29.67	29.59
F$_3$	68.04	40.16	57.58	69.50	63.39

Using Eq. (6), proposed by Coats and Redfern, the activation energy for every $g(\alpha)$ listed in Table 1 can be obtained at constant heating rates from fitting of $\ln(g(\alpha)/T^2)$ *vs.* $1000/T$ plots. For this study we have used the same conversion values as those used in the previous methods.

Tables 3–6 show activation energies at constant heating rate values: 5, 15, 25, 35 and 45°C min^{-1} for the different systems studied. The correlations were better than 0.99 in all cases [18–21]. Analysis of these tables suggests that the solid state thermo-degradation mechanisms which follow the systems not immersed in HCl are sigmoidal type (A_4 for the system without filler and A_2 for the system with filler).

The solid state thermodegradation mechanisms which follow immersed epoxy systems are decelerated (F_1; R_n) type for the system without filler and D_n type for the system with filler.

To check if the thermodegradation curves followed by the epoxy systems were the above-mentioned ones, we have used the method proposed by Criado *et al.* [3]. This method uses reference theoretical curves called master plots which are compared to experimental data. Experimental results are obtained from Eq. (7) at the optimum heating rate for each system, chosen through studies based on integral methods [18–21].
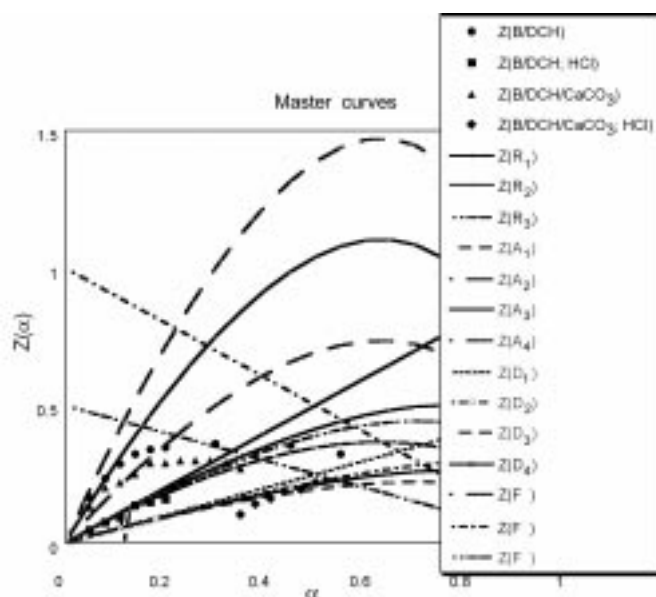

Fig. 7 Comparison between theoretical master plots corresponding to the different
solid state thermodegradation mechanisms and experimental master curves for
the immersed (Z(2; HCl) and Z(4; CaCO₃; HCl) and not immersed (Z(1) and
Z(3; CaCO₃) epoxy systems studied

Figure 7 shows master curve plots $Z(\alpha)$ *vs.* α, showing that, in the range of conversions used for this study, the better agreement between experimental results and Z

master curves corresponds to a sigmoidal mechanism for the systems not immersed in HCl and deceleration curves for the other systems.

Conclusions

For the two- and three-component systems studied, the internal structure of the epoxy network was affected neither by the presence of calcium carbonate filler nor by the immersion in hydrochloric acid, as the action of HCl on the three-component system was only on the surface.

After 30 days immersed in HCl, the activation energy calculated by Flynn–Wall–Ozawa method was not affected by the addition of calcium carbonate filler.

For the systems not immersed in hydrochloric acid the reaction mechanisms keep sigmoidal type (A_4 and A_2) and for the same systems immersed in hydrochloric acid the mechanisms change to deceleration curves (R_n and D_n).

References

 1 L. Núñez, F. Fraga, L. Fraga and J. A. Rodríguez, J. Thermal Anal., 47 (1996) 743.
 2 T. Hatakeyama and F. X. Quinn, 'Thermal Analysis Fundamentals and Applications to Polymer Science', Ed. J. Wiley & Sons, England 1994.
 3 J. M. Criado, J. Málek and A. Ortega, Thermochim. Acta, 147 (1989) 377.
 4 S. Montserrat, J. Málek and P. Colomer, Thermochim. Acta, 313 (1998) 83.
 5 S. Ma, J. O. Hill and S. Heng, J. Thermal Anal., 37 (1991) 1161.
 6 J. Šesták and G. Berggren, Thermochim. Acta, 3 (1971) 1.
 7 H. E. Kissinger, Anal. Chem., 29 (1957) 1702.
 8 J. H. Flynn and L. A. Wall, J. Res. Nat. Bur. Standards A Phys. Chem., 70A (1996) 487.
 9 T. Ozawa, Bull. Chem. Soc., Japan 38 (1965) 1881.
10 C. D. Doyle, Nature, 207 (1965) 240.
11 A. W. Coats and J. P. Redfern, Nature, 207 (1965) 290.
12 G. I. Senum and K. T. Yang, J. Thermal Anal., 11 (1977) 445.
13 H. Lee and K. Neville, 'Handbook of Epoxy Resin', McGraw–Hill, New York 1967.
14 C. A. May, 'Epoxy Resins: Chemistry and Technology', Marcel Dekker, New York 1988.
15 L. Núñez, F. Fraga, M. R. Núñez and M. Villanueva, J. Appl. Polym. Sci., 70 (1998) 1931.
16 L. Núñez, F. Fraga, A. Castro, M. R. Núñez and M. Villanueva, J. Appl. Polym. Sci., 75 (2000) 291.
17 L. Núñez, F. Fraga, A. Castro, M. R. Núñez and M. Villanueva, Polymer, 42 (2001) 3581.
18 L. Núñez, F. Fraga, M. R. Núñez and M. Villanueva, Polymer, 41 (2000) 4635.
19 M. Rosa Núñez Pardo de Vera, PhD Thesis, University of Santiago de Compostela, 1999.
20 A. M. Castro Bralo, PhD Thesis, University of Santiago de Compostela, 1999.
21 B. Rial Guldrís, MSc Thesis, University of Santiago de Compostela, 2000.
22 A. Jimenez, V. Berenguer, J. López and A. Sanchez, J. Appl. Polym. Sci., 50 (1993) 1565.
23 L. A. Pérez-Maqueda, A. Ortega and J. M. Criado, Thermochim. Acta, 277 (1996) 165.